SLAC-PUB-7595
August 15, 1997

A Preliminary Inclusive Measurement of A_c using the SLD Detector

The SLD Collaboration*

Stanford Linear Accelerator Center

Stanford University, Stanford, CA 94309

Abstract

We report a new measurement of A_c using data obtained by SLD in 1993-1995. This measurement uses a vertex tag technique, where the selection of a c hemisphere is based on the reconstructed mass of the charm hadron decay vertex. The method uses the 3D vertexing capabilities of SLD's CCD vertex detector and the small and stable SLC beams to obtain a high hemisphere c-tagging efficiency and purity of 13% and 69%, respectively. Charged kaons identified by the CRID detector and the charge of the reconstructed vertex provide an efficient quark-antiquark tag. We obtain a preliminary 93-95 result of $A_c = 0.662 \pm 0.068 \pm 0.042$

Contributed to the XVIII Symposium on Lepton Photon Interactions, July 28 - August 1 1997, Hamburg, Germany,
and to the International Europhysics Conference on High Energy Physics, 19-26 August 1997, Jerusalem, Israel. EPS-126

1 Introduction

Measurements of fermion asymmetries at the Z^0 resonance probe a combination of the vector and axial vector couplings of the Z^0 to fermions, $A_f = 2v_f a_f/(v_f^2 + a_f^2)$. The parameters A_f express the extent of parity violation at the Zff vertex and provide sensitive tests of the Standard Model.

The Born-level differential cross section for the reaction $e^+e^- \to Z^0 \to f\bar{f}$ is

$$d\sigma_f \,/\, dz \propto (1 - A_e P_e)(1 + z^2) + 2A_f(A_e - P_e)z\,, \tag{1}$$

where P_e is the longitudinal polarization of the electron beam ($P_e > 0$ for right-handed (R) polarization) and $z = \cos\theta$ is the direction of the outgoing fermion relative to the incident electron. The parameter A_f can be isolated by forming the left-right forward-backward asymmetry $\tilde{A}^f_{FB}(z) = |P_e| A_f\, 2z/(1 + z^2)$, although in this analysis we work directly with the basic cross section.

2 The SLD Detector

The operation of the SLAC Linear Collider with a polarized electron beam has been described in detail elsewhere [1]. During the 1994-95 run, the SLC Large Detector (SLD) [2] recorded 100k hadronic Z^0 decays with a luminosity-weighted electron beam polarization of $|P_e| = 0.773 \pm 0.006$. In 1993 a sample of 50k events with average polarization of $|P_e| = 0.623 \pm 0.011$ was obtained.

Charged particle tracking and momentum analysis is provided by the Central Drift Chamber [3] and the CCD-based vertex detector [4], with combined momentum resolution $\delta p_\perp/p_\perp = \sqrt{(.01)^2 + (.0026\; p_\perp/GeV)^2}$ in the plane perpendicular to the beam axis. The Liquid Argon Calorimeter (LAC) [5] measures the energies of charged and neutral particles and is also used for electron identification. Muon tracking is provided by the Warm Iron Calorimeter (WIC) [6]. The Cherenkov Ring Imaging Detector (CRID) [7] information (limited to the barrel region) provides the kaon identification. It consists of liquid and gas Cherenkov radiators illuminating a large area UV photon detectors. Only the gas information has been included in this analysis, since the liquid covers only marginally the interesting momentum region.

3 Event Selection

Hadronic events are selected based on the visible energy and track multiplicity in the event. The visible energy is measured using central drift chamber (CDC) tracks and must exceed

18GeV. There must be at least 7 CDC tracks, 3 that associate to hits in the vertex detector. We also require that the thrust axis, measured from calorimeter clusters, satisfy $|cos\theta| < 0.71$. This insures that the event is contained well within the acceptance of the vertex detector. All detector elements are also required to be fully operational. Additionally, we restrict events to 3 jets or less to make sure that we have well defined hemispheres. Jets being defined by the JADE algorithm [8] with a $ycut = 0.02$ A total of 83K events pass the above hadronic event selection and jet cut. Background, predominately due to taus, is estimated at $< 0.1\%$.

The SLC interaction point (IP) has a size of approximately $(1.5 \times 0.5 \times 700)\mu m$ in (x,y,z). The motion of the IP xy position over a short time interval is estimated to be $6\mu m$. Since this motion is smaller than the xy resolution for fitting tracks to find the primary vertex (PV) in a given event, we use the average IP position, for the x and y coordinates of the primary vertex. The average is obtained from tracks with hits in the vertex detector in 30 sequential hadronic events. The z coordinate of the PV is determine from each event separately. This results in a PV uncertainty of $7\mu m$ transverse and $35\mu m$ longitudinally to the beam direction.

3.1 Track Selection

Reconstruction of the mass of heavy hadrons is preceded by first identifying secondary vertices in each hemisphere. Only tracks that are well measured are included in the vertex and mass reconstruction. Tracks are required to have at least 40 CDC hits and start within a radius of 39cm of the IP. The CDC track is also required to extrapolate to within 1cm of the IP in xy and within 1.5cm of the PV in z. At least two vertex detector hits are required, the combined drift chamber + vertex detector fit must satisfy $\chi^2/d.o.f. < 5$, and $|cos\theta| < 0.8$. Tracks with an xy impact parameter > 3.0mm or an xy impact parameter error $> 250\mu m$ with respect to the IP are removed from consideration in the vertex and mass reconstruction.

3.2 Vertex Mass Reconstruction

Vertex identification is done using a topological vertexing method [9]. This method searches for space points in 3D where track density functions overlap. Each track is parameterized by a Gaussian density tube with a width equal to the uncertainty in the measured track position at the IP. Points in space where there is a large probable overlap of Gaussian tubes is considered as a possible vertex point. Determination of a vertex is done by clustering maxima in the overlap density distribution into vertices for separate hemispheres. We found secondary vertices in 50% of b, 16% of charm, and less than 1% of light quark hemispheres.

Only vertices that are significantly displaced from the PV are considered to be possible B or D hadron decay vertices. We require a distance between the PV and secondary vertex of at least 1mm.

Due to the cascade nature of the B decay, tracks from the decay may not all originate from the same space point. Therefore, a process of attaching tracks to the secondary vertex has been developed based on the transverse and longitudinal distance of closest approach of the track to the PV-secondary vertex axis.

The mass of the secondary vertex is calculated using the tracks that are associated with the vertex, including the tracks that have been added. Each track is assigned the mass of the charged pion and the invariant mass of the vertex is then calculated. The reconstructed mass is corrected to account for neutral particles. Using kinematic information from the vertex flight path and the momentum sum of the tracks associated with the secondary vertex, we add a minimum amount of missing momentum to the invariant mass. This is done by assuming the true quark momentum is aligned with the flight direction of the vertex. The so called P_t corrected mass is given by:

$$M_c = \sqrt{{M^2}_{tk} + {P_t}^2} + |P_t|$$

where M_{tk} is the mass for the tracks associated with the secondary vertex. We restrict the contribution to the invariant mass that the additional transverse momentum adds to be less than the initial mass of the secondary vertex. This cut ensures that poorly measured vertices in *uds* events do not leak into the sample by adding in large P_t.

3.3 Flavor Tag

A bottom tag is defined as a hemisphere with an invariant mass above 2 GeV. The intermediate mass region, between 0.6 and 2 GeV contains a mixture of b and c, with a small *uds* background. We define some additional cuts to reject b and *uds*. A charm tag is defined as follows:

- $0.6 < M_c < 2$GeV
- Vertex momentum (P_V) greater than 5 GeV.
- Fragmentation cut: $15M_c - P_V < 10$. This uses the fact that D hadrons from charm have a higher momentum for the same mass than those from b quarks.
- One track with an impact parameter greater than 3σ. This cut reduces the *uds* background.
- Veto on a tagged b on the opposite hemisphere.

For charm, this tag selects one or both hemisphere in about 24% of the events. The tagged sample has a 69% charm purity.

3.4 Signal Tag

The tag that determines the direction of the quark has two components. The first one is the vertex charge, Q_V. Charged vertices, coming mostly from $D^{\pm}$ and D_s have a positive charge for c vertices and a negative charge for $\bar{c}$. One would expect that the b background has an opposite sign, but this is diluted significantly in reality. The b vertices that survive the charm tag usually miss some tracks and therefore have lost most of their quark anti-quark charge correlation information.

The second component is the kaon charge, Q_k. This is the total charge of the identified kaons in the vertex. For the kaon charge, the signals for $b \to c \to s$ and $c \to s$ decays have the same sign.

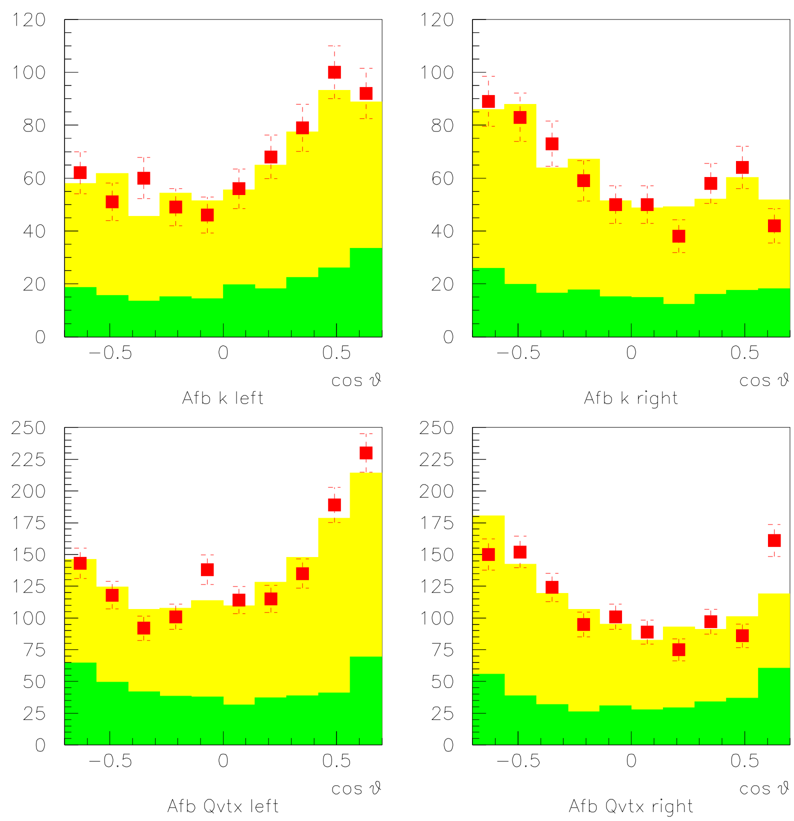

Figure 1: Measured asymmetry in the vertex charge and kaon channel for data (points) and MC (solid). The dark region indicated the non-charm background

For charm events, MC studies indicate a 33% efficiency for the kaon tag and 51% for the vertex charge. The correct tag probabilities are 82% and 85% respectively. For bottom events we have a 30% kaon efficiency with a 54% vertex charge efficiency, with correct tag probabilities for the two methods of 74% and 47% respectively. After this tag, our final sample is composed of 69% charm, 28% bottom and 3% *uds*. Both tags show a clear asymmetry signal as shown in fig 1.

4 Results

A maximum likelihood fit of all tagged hemispheres is used to determine A_c. As a likelihood function we use the total cross section.

$$L(p, P_e, z, A_b, A_c) \propto (1+z^2)(1-A_eP_e) + 2z(A_e - P_e) \quad (2)$$
$$\{F_b(p_{vtx})(1-2\chi)A_bC_b(tag) + F_c(p_{vtx})A_cC_c(tag) + F_{uds}A_{uds}\}$$

Here $F_{b,c,uds}$ is the probability to have a b, c, uds respectively for a hemisphere with vertex momentum p_{vtx}. The shape of the vertex momentum was taken from Monte Carlo, the overall normalization from the data. The factor $C_{b,c}$ (=$1-2P_{\text{wrong}}$) is the effectiveness of the tag, as given by Monte Carlo. This factor is taken to be independent of θ The quark direction is constructed from the thrust axis of the event, $z = -Q\cos\theta$. The three signs governing the left-right forward-backward asymmetry – beam polarization P_e, hemisphere tag charge Q, and quark direction $\cos\theta$ – are incorporated automatically into the maximum likelihood probability function.

A correction factor $(1-2\chi)$ is applied to all b-quark sources to account for asymmetry dilution due to $B^0\bar{B}^0$ mixing, with $\chi = .125$ taken from LEP measurements of the average mixing in $Z^0 \to b\bar{b}$ events [10]. The background asymmetry A_{bkg} is taken from MC simulation.

The QCD corrections to the cross-section are well known [11]. We take them info account with a correction term:

$$A^q_{FB|O(\alpha_s)}(\theta) = A^q_{FB|O(0)}(\theta)(1-\Delta^q_{O(\alpha_s)}(\theta))$$

These QCD correction have to be corrected for any bias in the analysis method to reject $q\bar{q}g$ events:

$$\Delta^{eff}_{\text{QCD}} = f\Delta_{\text{QCD}}$$

We estimate the analysis bias factor f for b and c from a Monte Carlo simulation at generator level:

$$f = \frac{A^{gen}_{q\bar{q}} - A^{analysis}_{\text{Parton Shower}}}{A^{gen}_{q\bar{q}} - A^{gen}_{\text{Parton Shower}}}$$

We found $f_c = 0.25 \pm 0.06$ and $f_b = 0.31 \pm 0.08$.

For 1993-1995 we find an efficiency of $\eta_c = 12.9 \pm 1.0\%$ for charm events, with a purity of $\pi_c = 69 \pm 2\%$. This agrees well with the Monte Carlo values of $\eta_c^{MC} = 12.6\%$ and $\pi_c^{MC} = 68\%$.

The background is made up of 3% uds and 28% b. From a sample of 83k selected events we measure A_c to be:

$$A_c = 0.662 \pm 0.068$$

This includes a QCD correction of $\Delta A_c = +0.009$.

5 Systematic Errors

The systematic errors can be found in table 1. We give a brief description of the different sources.

The tag composition is measured from the data [12]. Its statistical error contributes to the systematics, as does the uncertainty on the uds fraction from Monte Carlo and the uds asymmetry. We have used a 4% variation on the c fraction, 10% on the b fraction and 25% on the uds fraction. The uds asymmetry was found to be compatible with zero in the Monte Carlo. We use a value of 0.0 ± 0.5 to estimate the uncertainty from this source.

The fit systematics include the shape of the vertex momentum distributions and $\cos\theta$ dependence of the right-sign tagging probabilities and the tag composition. The former was estimated taking the difference between the MC momentum shape and a fit without momentum information. The latter was estimated from the difference between a constant value and a second order polynomial in $\cos\theta$ through the MC distributions of the tag composition and the tag effectiveness for all tags. We take the full difference as the systematic error.

The error from QCD corrections comes mainly from the uncertainty in the correction factors $f_{b,c}$. Gluon splitting and the error on α_s are also taken into account.

The vertex systematics are build up from detector sources and physics sources. For the detector we considered a 3% effect on the tracking efficiency. The dominant systematic error is the vertex smearing. This accounts for differences between Monte Carlo and data in the vertex charge distribution. These differences can be explained by assuming that there is a charge reconstruction problem. Smearing the charge distribution with a 7% probability of the secondary vertex tracks in the Monte Carlo to be absorbed in the primary vertex prduces a good agreement of the charge distribution between data and Monte Carlo. The full difference is taken as a systematic error.

The kaon related systematic errors come from two sources. The uncertainty in the kaon production ratios, and the actual kaon identification of the CRID detector. For the first we use the variations from [13] and for the second we vary the background misidentification level by 1σ. The misidenfication of pions as kaons is measured from data in K^0_S decays.

Another source of errors is the uncertainty in the production rates of the charmed hadrons. We vary them with the recommendation at the LEP Electroweak Working group [14].

Table 1: Systematic errors for the maximum likelihood analysis

source	δA_c
Tag Composition	
b,c, uds ratio	0.015
uds asymmetry (0.0 ± 0.5)	0.003
Fit Systematics	
Use p_D in fit vs not	0.002
$\cos\theta$ shape in P_D, tag	0.016
MC Statistics	0.006
QCD corrections	
Correction factor	0.004
α_s	0.001
$g \to c\bar{c}$	0.002
Vertex Charge	
Tracking efficiency 3%	0.016
Charge Smearing 7%	0.026
Kaon Systematics	
K mis-id	0.006
$D^{+/-}$ wrong sign K (0.81 $\pm$ 0.05)	0.005
D^0 wrong sign K (0.940 $\pm$ 0.013)	0.003
Physics Systematics	
D^+ ratio 0.259 ± 0.028	0.009
D_s ratio 0.115 ± 0.037	0.005
λ_c ratio 0.074 ± 0.029	0.001
$A_b(1-2\chi)$ (0.64 ± 0.11)	0.008
Polarization Systematics	
δP_e	0.005
$A_e = 0.152 \pm 0.008$	0.001
total	0.0423

6 Conclusions

We have performed a measurement of A_c using a new method that uses some of the unique features of the SLD detector. Our preliminary result based on 150K hadronic Z^0 is:

$$A_c = 0.662 \pm 0.068 \pm 0.042 \qquad \textbf{Preliminary}$$

This result is consistent with the SM expectation of 0.67 and other measurements at SLD and LEP. Due to the efficient tag and high analyzing power inclusive flavor separation, the statistical power of this analysis is significantly improved compared to more conventional techniques. This result is still statistically limited. and the systematic errors are small and mostly uncorrelated with those from existing methods. With a new data from the 1996 run of SLD, taken with an improved vertex detector, we expect a further reduction of the errors.

Acknowledgements

This work was supported by Department of Energy contracts: DE-FG02-91ER40676 (BU), DE-FG03-92ER40701 (CIT), DE-FG03-91ER40618 (UCSB), DE-FG03-92ER40689 (UCSC), DE-FG03-93ER40788 (CSU), DE-FG02-91ER40672 (Colorado), DE-FG02-91ER40677 (Illinois), DE-AC03-76SF00098 (LBL), DE-FG02-92ER40715 (Massachusetts), DE-AC02-76ER03069 (MIT), DE-FG06-85ER40224 (Oregon), DE-AC03-76SF00515 (SLAC), DE-FG05-91ER40627 (Tennessee), DE-AC02-76ER00881 (Wisconsin), DE-FG02-92ER40704 (Yale); National Science Foundation grants: PHY-91-13428 (UCSC), PHY-89-21320 (Columbia), PHY-92-04239 (Cincinnati), PHY-88-17930 (Rutgers), PHY-88-19316 (Vanderbilt), PHY-92-03212 (Washington); the UK Science and Engineering Research Council (Brunel and RAL); the Istituto Nazionale di Fisica Nucleare of Italy (Bologna, Ferrara, Frascati, Pisa, Padova, Perugia); and the Japan-US Cooperative Research Project on High Energy Physics (Nagoya, Tohoku).

References

[1] K. Abe *et al.*, Phys. Rev. Lett. **73**, 25 (1994).

[2] SLD Design Report, SLAC Report 273 (1984).

[3] M. Hildreth *et al.*, SLAC-PUB-6656 (1994), NIM A367, 111 (1995)

[4] G. Agnew *et al.*, SLAC-PUB-5906 (1992).

[5] D. Axen *et al.*, Nucl. Inst. Meth. **A328**, 472 (1993).

[6] A. Benvenuti *et al.*, Nucl. Inst. Meth. **A276**, 94 (1989); **A290**, 353 (1990).

[7] D. Aston *et al.*, SLAC-PUB-4795, Nucl. Inst. Meth. A283, 582 (1989); K. Abe *et al.*, SLAC-PUB-5214, (1990).

[8] W. Bartel *et el.*, Z. Phys. **C33**, 23 (1986).

[9] D. Jackson, *"A Topological Vertex Reconstruction Algorithm for Hadronic Jets"*, *Nucl. Inst. & Meth.* **A388** (1997) 247.

[10] ALEPH Collab., Z Phys. **C62**, 179 (1994); DELPHI Collab., Phys. Lett. **B276**, 536 (1992); OPAL Collab., Z. Phys. **C60**, 19 (1993); L3 Collab., Phys. Lett. **B292**, 434 (1992).

[11] J. B. Stav and H. A. Olsen, Trondheim U. Preprint 1994-17, (1994).

[12] K. Abe *et al.*, SLAC-PUB 7594, Submitted to this conference.

[13] S. Barlag *et al.* Z. Phys. C55, 383 (1992)

[14] The Lep Electroweak Working Group, *LEPHF/96-01* July 1996.

* List of Authors

K. Abe,(19) K. Abe,(29) I. Adam,(27) T. Akagi,(27) N. Allen,(4) W.W. Ash,(27) D. Aston,(27)
K.G. Baird,(16) C. Baltay,(33) H.R. Band,(32) M.B. Barakat,(33) O. Bardon,(16)
T. Barklow,(27) A.O. Bazarko,(11) R. Ben-David,(33) A.C. Benvenuti,(2) G.M. Bilei,(22)
D. Bisello,(21) G. Blaylock,(7) J.R. Bogart,(27) B. Bolen,(17) T. Bolton,(11) G.R. Bower,(27)
J.E. Brau,(20) M. Breidenbach,(27) W.M. Bugg,(28) D. Burke,(27) T.H. Burnett,(31)
P.N. Burrows,(16) W. Busza,(16) A. Calcaterra,(13) D.O. Caldwell,(6) D. Calloway,(27)
B. Camanzi,(12) M. Carpinelli,(23) R. Cassell,(27) R. Castaldi,(23) A. Castro,(21)
M. Cavalli-Sforza,(7) A. Chou,(27) E. Church,(31) H.O. Cohn,(28) J.A. Coller,(3) V. Cook,(31)
R. Cotton,(4) R.F. Cowan,(16) D.G. Coyne,(7) G. Crawford,(27) A. D'Oliveira,(8)
C.J.S. Damerell,(25) S. Dasu,(27) M. Daoudi,(27) N. De Groot,(27) R. De Sangro,(13)
R. Dell'Orso,(23) M. Dima,(9) P. Dervan,(4) D.N. Dong,(16) P.Y.C. Du,(28) R. Dubois,(27)
B.I. Eisenstein,(14) V. Onno Eschenburg,(18) E. Etzion,(32) S. Fahey,(10) D. Falciai,(22)
C. Fan,(10) M.J. Fero,(16) K. Flood,(17) R. Frey,(20) T. Gillman,(25) G. Gladding,(14)
S. Gonzalez,(16) E.L. Hart,(28) J.L. Harton,(9) A. Hasan,(4) Y. Hasegawa,(29) K. Hasuko,(29)
S. Hedges,(4) S.S. Hertzbach,(17) M.D. Hildreth,(27) J. Huber,(20) M.E. Huffer,(27)
E.W. Hughes,(27) X. Huynh,(27) H. Hwang,(20) Y. Iwasaki,(29) D. Jackson,(25) P. Jacques,(24)
J. Jaros,(27) A.S. Johnson,(3) J.R. Johnson,(32) R.A. Johnson,(8) T. Junk,(27)
R. Kajikawa,(19) M. Kalelkar,(24) Y. Kamyshkov,(28) H.J. Kang,(34) I. Karliner,(14)
H. Kawahara,(27) H.W. Kendall,(16) Y. Kim,(26) M.E. King,(27) R. King,(27) R.R. Kofler,(17)
N.M. Krishna,(10) R.S. Kroeger,(18) J.F. Labs,(27) M. Langston,(20) A. Lath,(16)
J.A. Lauber,(10) D.W.G. Leith,(27) V. Lia,(16) X. Liu,(7) M. Loreti,(21) A. Lu,(6)
H.L. Lynch,(27) J. Ma,(31) G. Mancinelli,(24) S. Manly,(33) G. Mantovani,(22)
T.W. Markiewicz,(27) T. Maruyama,(27) H. Masuda,(27) E. Mazzucato,(12)

A.K. McKemey,[4] B.T. Meadows,[8] G. Menegatti,[12] R. Messner,[27] P.M. Mockett,[31]
K.C. Moffeit,[27] T. Moore,[33] D. Muller,[27] T. Nagamine,[27] S. Narita,[29]
U. Nauenberg,[10] H. Neal,[27] M. Nussbaum,[8] Y. Ohnishi,[19] N. Oishi,[19]
D. Onoprienko,[28] L.S. Osborne,[16] R.S. Panvini,[30] H. Park,[20] C.H. Park,[35]
T.J. Pavel,[27] I. Peruzzi,[13] M. Piccolo,[13] L. Piemontese,[12] E. Pieroni,[23] K.T. Pitts,[20]
R.J. Plano,[24] R. Prepost,[32] C.Y. Prescott,[27] G.D. Punkar,[27] J. Quigley,[16]
B.N. Ratcliff,[27] T.W. Reeves,[30] J. Reidy,[18] P.L. Reinertsen,[7] P.E. Rensing,[27]
L.S. Rochester,[27] P.C. Rowson,[11] J.J. Russell,[27] O.H. Saxton,[27] T. Schalk,[7]
R.H. Schindler,[27] U. Schneekloth,[16] B.A. Schumm,[15] J. Schwiening,[27] S. Sen,[33]
V.V. Serbo,[32] M.H. Shaevitz,[11] J.T. Shank,[3] G. Shapiro,[15] D.J. Sherden,[27]
K.D. Shmakov,[28] C. Simopoulos,[27] N.B. Sinev,[20] S.R. Smith,[27] M.B. Smy,[9]
J.A. Snyder,[33] H. Staengle,[9] P. Stamer,[24] H. Steiner,[15] R. Steiner,[1] M.G. Strauss,[17]
D. Su,[27] F. Suekane,[29] A. Sugiyama,[19] S. Suzuki,[19] M. Swartz,[27] A. Szumilo,[31]
T. Takahashi,[27] F.E. Taylor,[16] E. Torrence,[16] A.I. Trandafir,[17] J.D. Turk,[33]
T. Usher,[27] C. Vannini,[xx] J. Va'vra,[27] C. Vannini,[23] E. Vella,[27] J.P. Venuti,[30]
R. Verdier,[16] P.G. Verdini,[23] S.R. Wagner,[27] D.L. Wagner,[10] A.P. Waite,[27]
J. Wang,[27] C. Ward,[4] S.J. Watts,[4] A.W. Weidemann,[28] E.R. Weiss,[31]
J.S. Whitaker,[3] S.L. White,[28] F.J. Wickens,[25] D.C. Williams,[16] S.H. Williams,[27]
S. Willocq,[27] R.J. Wilson,[9] W.J. Wisniewski,[5] M. Woods,[27] G.B. Word,[24]
T.R. Wright,[32] J. Wyss,[21] R.K. Yamamoto,[16] J.M. Yamartino,[16] X. Yang,[20]
J. Yashima,[29] S.J. Yellin,[6] C.C. Young,[27] H. Yuta,[29] G. Zapalac,[32] R.W. Zdarko,[27]
and J. Zhou[20]

[1] Adelphi University, Garden City, New York 11530
[2] INFN Sezione di Bologna, I-40126 Bologna, Italy
[3] Boston University, Boston, Massachusetts 02215
[4] Brunel University, Uxbridge, Middlesex UB8 3PH, United Kingdom
[5] California Institute of Technology, Pasadena, California 91125
[6] University of California at Santa Barbara, Santa Barbara, California 93106
[7] University of California at Santa Cruz, Santa Cruz, California 95064
[8] University of Cincinnati, Cincinnati, Ohio 45221
[9] Colorado State University, Fort Collins, Colorado 80523
[10] University of Colorado, Boulder, Colorado 80309
[11] Columbia University, New York, New York 10027
[12] INFN Sezione di Ferrara and Università di Ferrara, I-44100 Ferrara, Italy
[13] INFN Lab. Nazionali di Frascati, I-00044 Frascati, Italy
[14] University of Illinois, Urbana, Illinois 61801
[15] Lawrence Berkeley Laboratory, University of California, Berkeley, California 94720
[16] Massachusetts Institute of Technology, Cambridge, Massachusetts 02139
[17] University of Massachusetts, Amherst, Massachusetts 01003
[18] University of Mississippi, University, Mississippi 38677
[19] Nagoya University, Chikusa-ku, Nagoya 464 Japan
[20] University of Oregon, Eugene, Oregon 97403

[21] INFN Sezione di Padova and Università di Padova, I-35100 Padova, Italy
[22] INFN Sezione di Perugia and Università di Perugia, I-06100 Perugia, Italy
[23] INFN Sezione di Pisa and Università di Pisa, I-56100 Pisa, Italy
[24] Rutgers University, Piscataway, New Jersey 08855
[25] Rutherford Appleton Laboratory, Chilton, Didcot, Oxon OX11 0QX United Kingdom
[26] Sogang University, Seoul, Korea
[27] Stanford Linear Accelerator Center, Stanford University, Stanford, California 94309
[28] University of Tennessee, Knoxville, Tennessee 37996
[29] Tohoku University, Sendai 980 Japan
[30] Vanderbilt University, Nashville, Tennessee 37235
[31] University of Washington, Seattle, Washington 98195
[32] University of Wisconsin, Madison, Wisconsin 53706
[33] Yale University, New Haven, Connecticut 06511
[34] Sogang University, Seoul, Korea
[35] Soongsil University, Seoul, Korea